INTERNATIONAL JOURNAL OF
RADIATION ONCOLOGY • BIOLOGY • PHYSICS
www.redjournal.org

BIOLOGY CONTRIBUTION

Irradiation with Carbon Ions Effectively Counteracts Hypoxia-related Radioresistance in a Rat Prostate Carcinoma

Christin Glowa, PhD,[*,†,‡] Alina L. Bendinger, PhD,[†,‡,§] Rosemarie Euler-Lange, BSc,[†,‡,‖] Peter Peschke, PhD,[†,‡] Stephan Brons, PhD,[‡,¶] Jürgen Debus, MD, PhD,[*,‡,#] and Christian P. Karger, PhD[†,‡]

[*]*Department of Radiation Oncology and Radiotherapy, University Hospital Heidelberg, Heidelberg, Germany;* [†]*Department of Medical Physics in Radiation Oncology, German Cancer Research Center (DKFZ), Heidelberg, Germany;* [‡]*Heidelberg Institute for Radiation Oncology (HIRO), National Center for Radiation Research in Oncology (NCRO), Heidelberg, Germany;* [§]*University of Heidelberg, Faculty of Biosciences, Heidelberg, Germany;* [‖]*Department of Radiooncology/Radiobiology, German Cancer Research Center (DKFZ), Heidelberg, Germany;* [¶]*Heidelberg Ion Beam Therapy Center (HIT), Heidelberg, Germany; and* [#]*Clinical Cooperation Unit Radiation Therapy, German Cancer Research Center (DKFZ), Heidelberg, Germany*

Received Jan 8, 2024; Accepted for publication May 6, 2024

Purpose: Hypoxia in tumors is associated with increased malignancy and resistance to conventional photon radiation therapy. This study investigated the potential of particle therapy to counteract radioresistance in syngeneic rat prostate carcinoma.

Methods and Materials: Subcutaneously transplanted R3327-HI tumors were irradiated with photons or carbon ions under acute hypoxic conditions, induced by clamping the tumor-supplying artery 10 min before and during irradiation. Dose-response curves were determined for the endpoint "local tumor control within 300 days" and compared with previously published data acquired under oxic conditions. Doses at 50% tumor control probability (TCD_{50}) were used to quantify hypoxia-induced radioresistance relative to that under oxic conditions and also to quantify the increased effectiveness of carbon ions under oxic and hypoxic conditions relative to photons.

Results: Compared with those under oxic conditions, TCD_{50} values under hypoxic conditions increased by a factor of 1.53 ± 0.08 for photons and by a factor of 1.28 ± 0.06 for carbon ions (oxygen enhancement ratio). Compared with those for photons, TCD_{50} values for carbon ions decreased by a factor of 2.08 ± 0.13 under oxic conditions and by a factor of 2.49 ± 0.08 under hypoxic conditions (relative biological effectiveness). While the slope of the photon dose-response curves increased when changing from oxic to hypoxic conditions, the slopes were steeper and remained unchanged for carbon ions.

Conclusions: The reduced oxygen enhancement ratio of carbon ions indicated that the required dose increase in hypoxic tumors was 17% lower for carbon ions than for photons. Additionally, carbon ions reduced the effect of intertumor heterogeneity on the radiation response. Therefore, carbon ions may confer a significant advantage for the treatment of hypoxic tumors

Corresponding author: Christian P. Karger, PhD; E-mail: c.karger@dkfz.de

Disclosures: C.G. reports grants from the German Research Foundation (DFG) for the submitted work. J.D. reports grants from RaySearch Laboratories AB, Vision RT Limited, Merck Serono GmbH, Siemens Health Care GmbH, PTW-Freiburg Dr Pychlau GmbH, and Accuray Incorporated outside the submitted work. C.P.K. reports grants from the German Research Foundation (DFG) for the submitted work and from the German Cancer Aid (DKH) outside the submitted work. All other authors declare no potential conflicts of interest.

Data Sharing Statement: Research data will be shared upon request to the corresponding author.

Acknowledgments—We gratefully acknowledge the excellent experimental conditions provided by the Heidelberg Ion Beam Therapy Center (HIT), the Center for Preclinical Research (ZPF) at the German Cancer Research Center (DKFZ), and the Small Animal Imaging Core Facility of DKFZ. This work was funded by the German Research Foundation (DFG, GL 893/1-2 and KA 2679/3-2).

Supplementary material associated with this article can be found in the online version at doi:10.1016/j.ijrobp.2024.05.004.

Int J Radiation Oncol Biol Phys, Vol. 120, No. 3, pp. 875–883, 2024
0360-3016/$ - see front matter
https://doi.org/10.1016/j.ijrobp.2024.05.004

Introduction

Regions of low oxygen concentration (hypoxia) are a common feature of many solid malignancies and result from an imbalance between oxygen delivery and consumption. The transport of oxygen to neoplastic and stromal cells is frequently reduced or abolished by severe structural abnormalities in tumor vessels, deteriorated diffusion geometry, and disturbed microcirculation.[1,2] Hypoxia-inducible factor-1α is considered the major transcription factor that activates signaling pathways regulating proliferation, angiogenesis, energy metabolism, pH, DNA damage repair, genetic instability, tissue invasion, and metastasis, as well as cancer stem cell maintenance and reprogramming.[3] These induced biologic processes allow cancer cells to adapt, survive, and grow under hypoxic conditions. Hence, tumor hypoxia is recognized as a major aspect of malignant progression, poor prognosis, and resistance to therapy.[1,2,4,5] Hence, the ability to identify hypoxic tumors, the development of strategies to overcome hypoxia, and the enhancement of therapeutic efficacy remain important goals in oncological research.

Although preclinical imaging techniques to assess tumor hypoxia that have potential for clinical implementation are available,[6-8] successful treatment of hypoxic tumors remains a clinically relevant problem, especially in radiation therapy. For decades, hypoxic cells have been documented to be more radioresistant, owing to the reduced fixation of DNA lesions, higher mobilization of the antioxidant defense network, and hypoxia-induced activation of survival factors.[9-11] The effect of oxygen in sensitizing cells to radiation is quantified by the so-called "oxygen enhancement ratio" (OER), given as the ratio of doses in the absence (D_{hyp}) and presence (D_{ox}) of oxygen needed to obtain the same biologic effect. In the definition of OER, the dose D_{hyp} under completely hypoxic conditions was used as a reference, whereas D_{ox} depends on the actual oxygen partial pressure (pO_2).

Various therapeutic approaches to overcome hypoxia have been evaluated.[12] Ion beams with high linear energy transfer (LET) have been used to treat radioresistant tumors.[13] Besides an increased "relative biological effectiveness" (RBE), defined as the ratio of photon and ion doses that lead to the same biologic effect,[14] it has been observed that cell inactivation by high-LET radiation is less dependent on oxygen than that by low-LET photon beams.[15] In vitro, this was demonstrated by a decreased OER in different cell lines after high-LET irradiation.[16] Several ion beam therapy centers worldwide offer high-LET carbon ion (^{12}C) irradiation as an additional strategy to treat cancer.[17] In contrast to photons, the inverse depth-dose profile of ions, as well as their energy-dependent finite range, allows for a higher dose prescription to the tumor, while reducing the dose in the surrounding normal tissue.[18] New developments, such as the active beam scanning and energy modulation technique, result in further dose conformation to the target and may even be used to boost the effectiveness in hypoxic subvolumes of the tumor by "dose- or LET-painting."[19-21]

Very little quantitative in vivo data are available on the sensitizing effect of carbon ions relative to photon beams in hypoxic tumors. In an early study, the OER was measured in the 9L glioma model, revealing values of 2.0 and 1.7 for the carbon ion plateau and spread-out Bragg-peak (SOBP) regions, respectively, in comparison to 2.1 for x-rays.[22] This study was extended to the R2D2 rhabdomyosarcoma model, revealing an OER in the carbon ion SOBP of 1.9, relative to 2.2 for x-rays.[23] In both studies, ambient and hypoxic conditions during irradiation were realized by air and nitrogen gassing of tumor-bearing animals, respectively. More recently, squamous cell carcinoma (SCCVII) tumors were irradiated with either carbon ions or x-rays under clamped or ambient conditions, respectively, and OER values of 1.87 ± 0.13 for x-rays, 1.43 ± 0.19 for the proximal position of the tumor, and 1.52 ± 0.10 for the distal position of the tumor in the carbon ion SOBP were obtained.[24] Although the tumor was irradiated in vivo in all these studies, the radiation response was analyzed only in vitro by colony formation assay immediately after irradiation and thus does not include the long-term interaction with the tumor microenvironment or the therapeutic outcome.

In the present study, the role of high-LET carbon ions in overcoming acute hypoxia-induced radiation resistance was evaluated for the first time fully in vivo using a syngeneic prostate tumor model together with the clinically relevant biologic endpoint local tumor control. The results demonstrated a reduced effect of hypoxia on the response to carbon ion irradiation compared with conventional photon treatments under realistic conditions.

Methods and Materials

Tumor model

Fresh fragments of tumor tissue from the syngeneic Dunning prostate adenocarcinoma R3327-HI[25] were implanted subcutaneously in the distal thigh of young adult male Copenhagen rats (age, 10 ± 2 weeks; weight, 180-200 g; Charles River LaboratoriesDuring irradiation, the rats were kept under inhalation anesthesia with a mixture of 2.5% sevoflurane (Abbott) and oxygen at 2 L/min using an inhalation mask. All experiments were approved by the government review committee for animal care (Ref. No. 35-9185.81/G-171/09 and 35-9185.81/G-88/14). The animals were kept under standard laboratory conditions.

Table 1 Dose levels and number of animals irradiated under clamping conditions

Experiment	Dose levels (Gy) (animals/dose level)	Animals
Photons	75 (4), 80 (5), 85 (6), 90 (6), 95 (7*), 100 (6), 105 (7*), 110 (3)	44
Carbon ions	27.0 (3), 29.5 (3), 32.0 (6), 34.5 (6), 37.0 (6), 39.5 (6), 42.0 (6), 44.5 (3)	39
Controls	5 sham-treated tumors per experimental arm	10
Total		**93**

* One animal died due to lymph node metastasis.

Irradiation and follow-up

Tumors from 93 animals were treated under acute hypoxic conditions using a single dose of photons or carbon ions (Table 1). Ten sham-treated animals served as controls. Hypoxia was induced by clamping the tumor-supplying artery 10 min before and during treatment. The effect of clamping on perfusion was validated by photoacoustic measurements.

The irradiation setup was the same as that used in a previous study on the same tumor performed under oxic conditions.[26] The rats were fixed in a special device for the accurate positioning of the tumor (see details in reference 27[27]). At treatment, the tumor diameter was 11 mm (range, 9.0-12.5 mm). Photon irradiation was performed using a single 6 MV beam of a linear accelerator (Siemens) at 300 MU/min, and the field size was shaped by a cylindrical tungsten collimator (90% isodose, 15 mm at the isocenter). For carbon ions, the tumor was positioned at the center of a single 20 mm SOBP with a field size of 18 × 18 mm^2 delivered by active raster scanning.[28] The mean dose-averaged LET in the tumor was 75 keV/μm (range, 64-96 keV/μm).[27] Total irradiation times were 7 min (carbon ions) and up to 30 min (photons). Figure 1 shows the tumor position within the photon and carbon ion depth-dose distributions.

Irradiation was performed with increasing doses in each experimental arm. The primary endpoint was "local tumor control within 300 days," defined as the absence of detectable tumor growth. As a few tumors regressed later, local tumor control within the extended follow-up period was used as the secondary endpoint. The tumor volume was measured routinely using a caliper.[27]

Quantitative analysis

For the primary endpoint (local tumor control), dose-response curves were fitted to the actuarial tumor control rates using the logistic dose-response model together with the maximum likelihood fitting procedure of the STATISTICA software.[29] The dose at 50% tumor control probability (TCD_{50}) was derived from the fit parameters (see references 27 and 30[27,30] for details). After adding data from a previous study performed under oxic conditions,[26] the OERs of photons and carbon ions were calculated as the ratio of the TCD_{50} values measured under hypoxic and oxic conditions.[14] The relative biological effectiveness (RBE) of carbon ions under hypoxic and oxic conditions was calculated as the ratio of the TCD_{50} values for photons and carbon ions.[14]

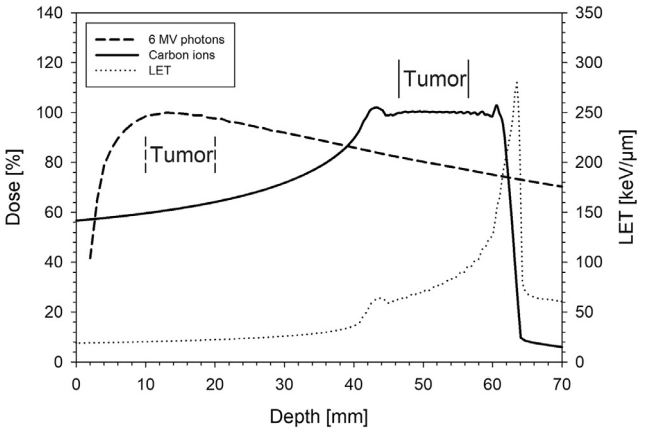

Fig. 1. Position of the tumor in the photon and carbon ion depth-dose distributions. The linear energy transfer curve for carbon ions is additionally displayed.

Statistics

Incomplete follow-up of animals was considered in the fitting procedure, using the method of effective sample sizes that corrects the number of treated and responding tumors to match actuarial response rates and their variances.[31] The standard errors of the TCD_{50}, OER, and RBE were calculated using error propagation. For the TCD_{50}, the correlation of the fit parameters was considered based on their covariance. Additionally, 90% confidence intervals were calculated using Fieller's theorem.[32]

Photoacoustic imaging

Photoacoustic imaging (PAI) in 2 tumor-bearing rats was used to assess pixel-based oxygen saturation (sO_2) distributions in HI tumors under oxygen-breathing conditions before clamping, 10 min after clamping induction, and 2 min after clamping release to confirm complete hypoxic conditions induced by clamping of the tumor-supplying arteries and reoxygenation after clamping release. For PAI measurements, the skin of the animals was thoroughly depilated using hair removal cream (Abbvie). During PAI, animals were anaesthetized with a mixture of 3% sevoflurane (Abbott) and oxygen at 1.0 L/min and placed on a heatable table. Ultrasound gel was applied to the entire accessible tumor surface to avoid air bubbles. PAI measurements were conducted with a Vevo3100 (Fujifilm VisualSonics Inc) using a tunable Nd:YAG laser (Vevo LAZR, Fujifilm

VisualSonics Inc) and a 21 MHz ultrasound transducer MX250 (Fujifilm VisualSonics Inc). PAI data were acquired in the 3-dimensional (3D) "oxy-hemo" mode to detect deoxygenated and oxygenated hemoglobin at 750- and 850-nm excitation wavelengths, respectively. The sO_2-distribution was measured when the animal was breathing oxygen, 10 min after clamping the tumor-supplying arteries, and 2 min after clamping release. The detailed PAI setup and analysis parameters have been published previously.[33]

Immunohistochemistry

To validate that the clamping procedure does not alter morphologic and functional characteristics of the tumor, immunohistochemistry was performed without clamping (3 animals) and 24 h after the clamping of the tumor was released (3 animals). Clamping was applied for 20 min to mimic the situation of carbon ion irradiation under clamping conditions (10 min clamping + 10 min sham irradiation). For marker injections, animals were kept under isoflurane (Baxter) anesthesia (3% isoflurane in 2 L/min oxygen). Animals were injected intraperitoneally with bromodeoxyuridine (BrdU; 100 mg/kg, 8 h, intraperitoneally, Sigma-Aldrichand pimonidazole hydrochloride (60 mg/kg, 1 h, intravenously, Hypoxyprobe-1 Kit, NPI Inc) before sacrifice. Hoechst 33342 dye (15 mg/kg, Merck KGaA, Darmstadt, Germany) was injected as a perfusion marker into the right ventricle of the heart 30 seconds before the tumors were dissected and stored at -80°C. Tumors were then embedded in Tissue Tek (Sakuracut into 7 μm thin slices, fixed in methanol/acetone, and stored at -20°C. Five minutes of hematoxylin/eosin (H&E; Carl Roth GmbH & Co KG) staining was used to evaluate tumor tissue structures.

Immunofluorescence staining was performed to detect pimonidazole, CD31, and BrdU. After blocking against nonspecific binding (Dako North America Inc), proliferating cells were stained with a BrdU antibody (Roche Diagnostics, Mannheim, Germany), and hypoxic areas were stained with FITC-labeled mouse antipimonidazole antibody (1:2000) in 3% bovine serum albumin/phosphate-buffered saline overnight at 4°C. The sections were then incubated with goat antirat CD31 antibody (1:2000, R&D Systems Inc. Minneapolis, MN) for 1 hour at room temperature and labeled with AlexaFluor-555 antibody (1:3000, 1 h, Invitrogen) to detect endothelial cells. Cell nuclei were counterstained with DAPI (Invitrogen AG, Carlsbad, CA), or perfused areas were detected via autofluorescence of the injected Hoechst 33342 dye. Sections were washed in phosphate-buffered saline, mounted in Fluoromount (Dako), and visualized using an Axio Scan.Z1 microscope (Carl Zeiss Microscopy GmbH, Jena, Germany).

Results

In this study, 93 animals were irradiated with either increasing single-fraction doses of 6 MV photons or carbon ions (Table 1) under hypoxic conditions induced by clamping the tumor-supplying arteries. Figure 1 shows the tumor positions in the photon and carbon ion depth-dose distributions.

To verify the effect of the clamping procedure on tumor oxygenation, PAI measurements in nonirradiated controls were performed before and during clamping, as well as shortly after clamping release. sO_2 histograms before clamping and after clamping release were nearly identical (red and green histograms) and exhibited a broad distribution with a clearly visible maximum at high sO_2 levels (Fig. 2A and Fig. E1A). In contrast, the distribution during clamping was reversed, showing a similar broad distribution but with a maximum at very low sO_2 levels. Figure 2B and Figure E1B display color maps of the sO_2 distribution at the 3 time points in the 2 HI tumors. Unirradiated control tumors, with or without clamping, showed similar growth patterns, tissue structures, proliferation, vessel density, hypoxia, and perfusion (Fig. 2C-H).

Figure 3 compares the dose-response curves for photons and carbon ions under hypoxic and oxic conditions. The corresponding TCD_{50}, OER, and RBE values are presented in Table 2. In all experimental arms, a tumor control rate of 100% was achieved. Hypoxic curves shifted to significantly higher doses. This shift was much larger for photons than for carbon ions, expressed by OER values of 1.53 and 1.28, respectively. While the slope of the photon curves increased when changing from oxic to hypoxic conditions, both carbon ion curves had similar slopes and were slightly steeper than the photon curves under hypoxic conditions. Comparing the effectiveness of the 2 beam modalities, the curves for carbon ions shifted to significantly lower doses. This shift was much larger under hypoxic conditions than under oxic conditions, expressed by RBE values of 2.49 versus 2.08, respectively. Using the extended rather than the 300-day follow-up only led to minor differences, and the above results remained valid (Table 2). Figure 4 shows the relationship between the measured RBE and OER values with respect to the tumor response.

Discussion

The prevalence of hypoxia in many solid tumors and its negative effect on treatment outcomes in radiation therapy have been well established, and various strategies have been suggested to overcome this major obstacle.[12] Given that high-LET particles, such as carbon ions, induce a higher fraction of clustered DNA double-strand breaks and that the resulting biological effect is less dependent on oxygen concentration and proliferation status, it is expected that carbon ion doses are more effective in tumors than the same absorbed doses of photons.[26,34-36] This higher efficacy was expressed by RBE values significantly above 1. OER is the ratio of doses that produce the same biologic endpoint under completely hypoxic versus ambient conditions. Although OER values of up to 3 have been reported for photons in cell inactivation experiments, the impact of hypoxia

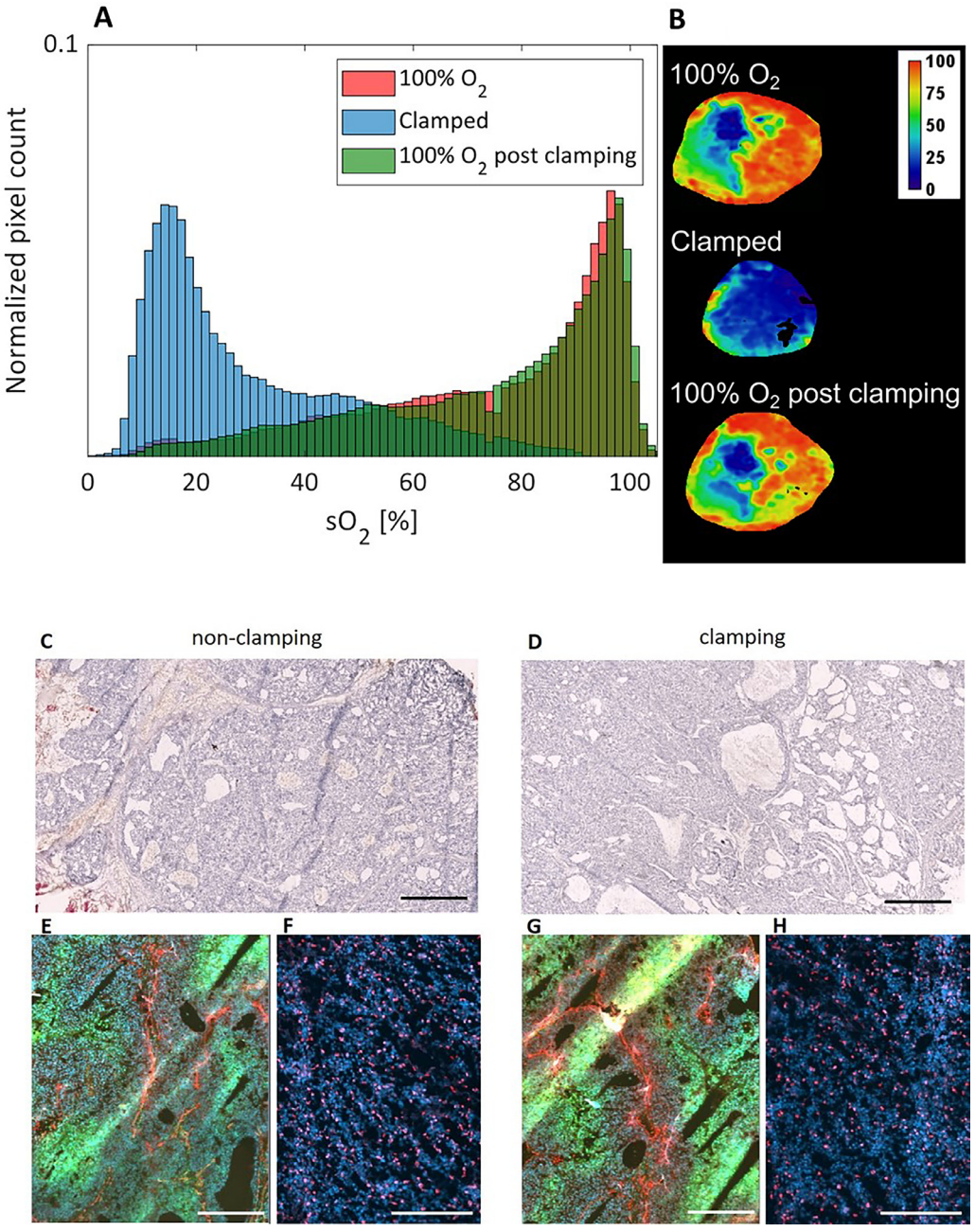

Fig. 2. Characterization of unirradiated tumors under clamping and nonclamping conditions. (A) Induction of acute hypoxia by clamping the tumor-supplying arteries validated by 3-dimensional (3D) photoacoustic imaging (PAI). Normalized sO_2 distributions for the first HI tumor prior to clamping (red histogram), after clamping the artery for 10 min (blue histogram), and 2 min after clamping release (green histogram) over the whole 3D tumor volume. (B) Representative sO_2 maps of the first tumor at the 3 time points (prior to and during clamping and after clamping release) from the PAI measurements. The position of the PAI probe is on the top side. The middle panel (clamped) shows a clear reduction in sO_2, while the preclamping distribution is restored after clamping release. The respective sO_2 distributions and sO_2 maps of the second investigated tumor are shown in Figure E1. (C-D) Histology staining shows typical structures of HI tumors, which were equal without clamping (C) and 24 h after clamping was released (D). (E, G) Immuno-fluorescence staining for vessels (CD31 in red), hypoxia (pimonidazole in green), and perfusion (Hoechst in blue) without clamping (E) and after clamping was released (G). (F, H) Immunofluorescence staining for proliferation (BrdU in red), and cell nuclei (DAPI in blue) without clamping (F) and after clamping was released (H). The clamping procedure revealed no structural differences for any of the fluorescence stainings. Scale bars, 1000 μm.

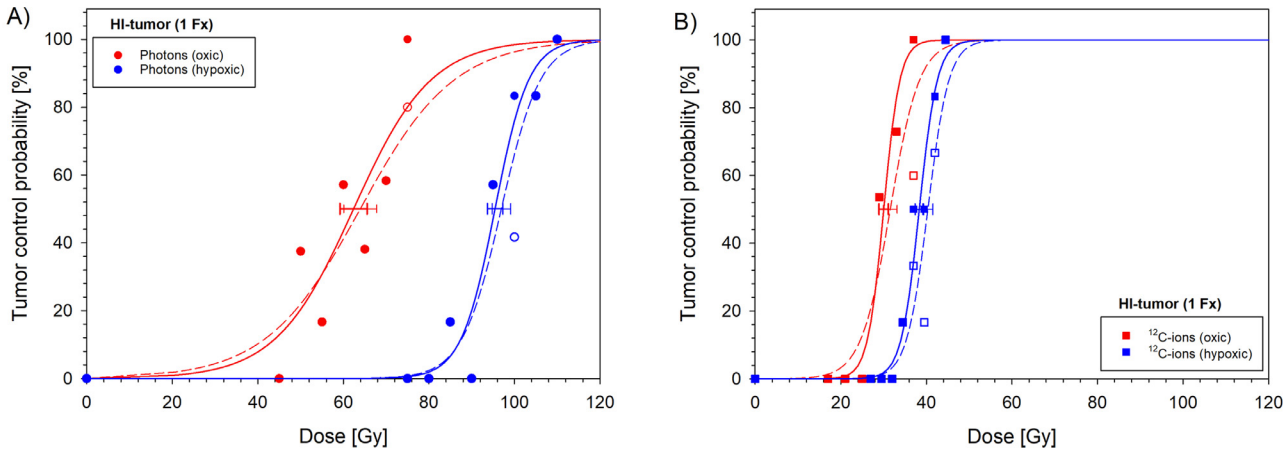

Fig. 3. Dose-response curves for photons (A) and carbon ions (B) measured under hypoxic conditions in comparison to the curves measured previously under oxic conditions.[26] Error bars (1 SE) indicate the uncertainty of the dose at 50% tumor control probability (TCD_{50}). Solid lines and closed symbols refer to the endpoint "local tumor control at 300 d after irradiation." Dashed lines and open symbols consider additional recurrences during the extended follow-up.

Table 2 TCD_{50}, OER, and RBE values measured in the present study

	TCD_{50} ± SE (90% CI) (Gy)		
Experiment	**Photons**	**Carbon ions**	**RBE ± SE (90% CI)**
300 d follow-up			
Hypoxic	95.5 ± 1.8 (92.2-98.9)	38.3 ± 1.0 (36.6-40.3)	**2.49 ± 0.08 (2.36-2.62)**
Oxic*	62.4 ± 3.2 (56.6-69.8)	30.0 ± 1.1 (27.5-32.6)	**2.08 ± 0.13 (1.87-2.30)**
OER ± SE (90% CI)	**1.53 ± 0.08 (1.40-1.68)**	**1.28 ± 0.06 (1.19-1.37)**	
Extended follow-up			
Hypoxic	97.0 ± 2.2 (93.3-101.6)	40.3 ± 1.2 (38.5-43.2)	**2.40 ± 0.09 (2.26-2.56)**
Oxic*	63.9 ± 3.9 (57.5-74.7)	31.6 ± 1.6 (28.7-35.5)	**2.03 ± 0.16 (1.78-2.30)**
OER ± SE (90% CI)	**1.52 ± 0.10 (1.37-1.69)**	**1.28 ± 0.08 (1.16-1.41)**	

* Data from reference 26.
While the OER measures the increased radioresistance under hypoxic relative to oxic conditions, the RBE measures the increased effectiveness of carbon ions relative to photons. Data for the oxic conditions were measured in a previous study.[26] Both studies were designed with a follow-up of 300 d. "Extended follow-up" additionally takes recurrences beyond 300 d into account. Uncertainties are provided as single standard errors and 90% confidence intervals.
Abbreviations: OER = oxygen enhancement ratio; RBE = relative biological effectiveness; TCD_{50} = dose at 50% tumor control probability.

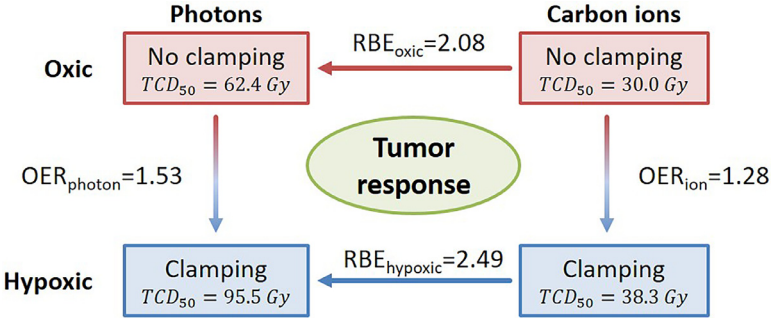

Fig. 4. Relation between hypoxia-induced radioresistance for photons and carbon ions expressed by the oxygen enhancement ratio (OER) and the increased effectiveness of carbon ions when the tumor is irradiated under oxic or hypoxic conditions as described by the relative biological effectiveness (RBE). Numerical values refer to the endpoint "local control at 300 d after irradiation."

on radioresistance is in the range of 1.5 to 2, and hence, is much smaller for high-LET irradiations.[15,16,20] Moreover, the oxygen effect is cell type−dependent, presumably owing to additional biological factors.[37] Using V79 spheroids instead of single cells, a relatively low OER of 1.4 was found for carbon ions in the SOBP, primarily evoked by a large amount of complex DNA damage, even under hypoxic conditions; however, it neglects the potential impact of vascular effects and the tumor microenvironment.[38,39]

In vivo, OER values are generally smaller but still well above 1. Although the impact of oxygenation on local tumor control has been investigated for photons,[40] all former studies with carbon ion beams irradiated tumor-bearing animals while the radiation response was analyzed only in vitro by colony formation assay immediately after irradiation, and thus, none of the experiments include the long-term interaction with the tumor microenvironment or the therapeutic outcome.[22-24] In this respect, the present study is the first full in vivo study with carbon ions providing OER values for the clinically most relevant endpoint "local tumor control," after a long-term follow-up of 300 days. The tumor subline R3327-HI used in this study represents a moderately well-differentiated prostate carcinoma with characteristics similar to many clinical tumors. This subline was selected because of its rather low hypoxic fraction[26] and its ability at larger volumes to reoxygenate under oxygen breathing,[41] which was also employed in our study. It could therefore be expected that clamping-induced hypoxia leads to a measurable difference in radiation response. That the clamping procedure actually reduced oxygenation in the tumor was validated by PAI,[33] and a previous study has demonstrated a positive correlation between the pO2 level in this tumor and growth delay after subtherapeutic doses.[41] Microscopically, the syngeneic rat prostate subline R3327-HI is characterized by a minor number of tubular prostate glands associated with wide immature vessels and irregular ring-like structures filled with large amounts of mucin. At the histologic level, both chronic hypoxic tumor cells, distantly located from vessels, as well as acute hypoxic cells in close proximity to unperfused vessels, were detected by immunofluorescence techniques.[42] The good agreement of the local tumor control probability curves for the 300-day and the extended follow-up times confirms that the 300-day follow-up is well suited to capture the recurrences for the selected prostate tumor.

Irradiations were performed under clamping conditions, which caused temporary (20 min) obstruction of the blood supply, where oxygen and nutrition supplies were abolished or greatly reduced.[43] Under the assumption that this short-term acute ischemic hypoxic state is the dominant physiological characteristic, most tumor cells will suffer a severe reduction in oxygen and nutrition but will not have enough time to effectively activate a wide range of molecular changes mediated by intracellular signaling pathways leading to survival under low oxygen conditions, as often seen in chronic hypoxic cells.[33,44] Hence, the physiological response to this transient technical manipulation, which was validated by photoacoustic measurements, did not show any effect on tumor growth, proliferation, vessel density, and perfusion in unirradiated tumors when clamping was released. It should be noted that besides PAI, other methods to monitor tumor oxygenation have been employed in the R3327-HI tumor, such as invasive pO2 histography,[45] ^{19}F-MRI relaxometry,[41] and the use of a fiber-optic oxygen sensor.[46] In previous studies, photoacoustic[47] as well as ^{19}F-MRI relaxometry[41] measurements showed a correlation between tumor oxygenation and tumor growth after irradiation.

Under these experimental conditions, the results of this study provide clear evidence that carbon ions effectively counteract the effect of hypoxia on the tumor response. Acute hypoxia increased the dose for local tumor control, TCD_{50}, by a factor (OER) of 1.53 for photon irradiation, while for carbon ions, a 17% lower OER of 1.28 was found. For tumors well supplied with oxygen, the higher effectiveness of carbon ions relative to photons resulted in an experimental RBE of 2.08. However, when the tumors were clamped, a 20% higher RBE of 2.49 was measured. As illustrated in Figure 4, this finding is a direct consequence of the lower OER of carbon ions relative to photons, which can be quantitatively expressed by

$$RBE_{hyp} = RBE_{ox} \cdot \frac{OER_{ph}}{OER_{ion}} \quad (1)$$

where RBE_{hyp} and RBE_{ox} refer to the RBE values under hypoxic and oxic conditions, respectively, and OER_{ph} and OER_{ion}, to the OER for photon and carbon ion irradiations, respectively. In the clinical situation, the benefit of carbon ions depends on the differential RBE between tumor and normal tissue rather than solely on the tumor RBE. However, since hypoxia is observed only in tumors but not in normal tissue, the response of the normal tissue remains unchanged for both radiation modalities if the tumor becomes hypoxic and if the same treatment field is applied. Thus, the RBE and RBE-weighted doses in the normal tissue do not change under hypoxic tumor conditions. As an important consequence, carbon ions deliver a 20% higher RBE−weighted dose to the tumor at the same complication risk. In contrast, a comparable escalation of tumor dose with photons would increase the dose to the normal tissue accordingly, thereby also increasing the risk of complications. This indicates a significant advantage of carbon ions over photons in the treatment of hypoxic tumors.

However, when translating our findings into the clinic, it has to be considered that the OER and RBE values found in this study refer to single rather than fractionated doses, as well as to a specific tumor type. Moreover, the selected tumor model and the applied clamping technique restrict the above results to "perfusion-limited" (acute) hypoxic conditions, while most solid tumors contain a mixture of acute and "diffusion-limited" (chronic) hypoxic cells. The latter is mainly a consequence of the limited diffusion of oxygen with tumor mass expansion, and the extended exposure of cells to this deprivation is characterized by changes in the DNA repair systems, metabolic conditions, proliferation status, and

development of microniches of quiescent cells. Additionally, the dynamics of oxygen fluctuations during hypoxia/reoxygenation cycles further complicate this situation, often leading to more pronounced radioresistance.[48,49] Finally, the presence of acute and/or chronic hypoxia, even under ambient conditions, may explain the generally lower in vivo OER values compared with those determined in vitro, where completely hypoxic and oxic conditions can easily be achieved.

The impact of carbon ions on overcoming hypoxia-induced radioresistance has also been demonstrated in 3 sublines of a tumor model differing in hypoxic status. The RBE increased from 1.62 to 2.30 when the hypoxic fraction (>10 mm Hg, HF_{10}) increased from 1% in a well-differentiated tumor to 18% in an anaplastic tumor, with the latter containing a reasonable number of chronic hypoxic cells. More generally, these experiments also showed that the large therapeutic differences often seen after photon therapy are considerably reduced by carbon ions, resulting in much steeper dose-response curves for carbon ions compared with photon treatments.[26] Interestingly, the slope of the dose-response curve for photons under clamping conditions also became much steeper, whereas the steep slope for carbon ions remained unchanged between oxic and hypoxic conditions. For the photon arm, this can be explained by oxygenation-related heterogeneity, which changed to a uniform hypoxic condition and thus to a reduced but uniform radiosensitivity under clamping conditions for all tumors. For carbon ions, the dependence on the individual oxygen status was already reduced by the high LET; thus, the homogenization of the oxygen level by clamping did not reveal any additional effect.

Solid tumors consist of large numbers of heterogeneous cancer cells, including a population of quiescent cancer cells residing in areas far from blood vessels. These cells are thought to arise because of long-lasting oxygen and nutrient deprivation and are considered to play an important role in cancer treatment failure.[11,50] In an ambitious in vivo/in vitro study, Masunaga et al showed in mice bearing mouse squamous cell carcinomas that high-LET carbon ions considerably decrease the radioresistance of intratumor quiescent cell populations, which contain a higher fraction of hypoxic cells than proliferating cell populations in solid tumors.[51] Finally, some indications were found in a clinical study, where individual pO_2 measurements in patients with cervical cancer before and during carbon ion treatment were correlated with disease-free survival and local tumor control rates, revealing that heavy-ion therapy reduces hypoxia-driven tumor radioresistance.[52]

The effectiveness of carbon ions is known to depend on physical parameters, such as ion type, LET, and dose, and this dependence is considered using biophysical models in treatment planning.[53-55] Quantitative models are not yet available for biological factors originating from the tumor itself or its microenvironment, and additional experimental investigations are necessary to determine the impact of these factors on clinically relevant endpoints. This study demonstrated, for the first time, the counteracting effect of carbon ions on hypoxia-induced radioresistance under conditions close to the clinical situation. Considering that hypoxia also alters angiogenesis, apoptosis, tumor metabolism, and immune responses,[44] as well as the progression and metastatic potential of prostate cancer[56], carbon ions are a promising treatment strategy to effectively counteract hypoxia-induced radioresistance.

References

1. Höckel M, Vaupel P. Tumor hypoxia: Definitions and current clinical, biologic, and molecular aspects. *J Natl Cancer Inst* 2001;93:266-276.
2. Harris AL. Hypoxia—a key regulatory factor in tumour growth. *Nat Rev Cancer* 2002;2:38-47.
3. Roy S, Kumaravel S, Sharma A, et al. Hypoxic tumor microenvironment: Implications for cancer therapy. *Exp Biol Med* 2020;245:1073-1086.
4. Ratcliffe PJ, O'Rourke JF, Maxwell PH, et al. Oxygen sensing, hypoxia-inducible factor-1 and the regulation of mammalian gene expression. *J Exp Biol* 1998;201:1153-1162.
5. Semenza GL. Targeting hif-1 for cancer therapy. *Nat Rev Cancer* 2003;3:721-732.
6. Tatum JL, Kelloff GJ, Gillies RJ, et al. Hypoxia: Importance in tumor biology, noninvasive measurement by imaging, and value of its measurement in the management of cancer therapy. *Int J Radiat Biol* 2006;82:699-757.
7. O'Connor JPB, Robinson SP, Waterton JC. Imaging tumour hypoxia with oxygen-enhanced mri and bold mri. *Br J Radiol* 2019;92 20180642.
8. Matsuo M, Matsumoto S, Mitchell JB, et al. Magnetic resonance imaging of the tumor microenvironment in radiotherapy: Perfusion, hypoxia, and metabolism. *Semin Radiat Oncol* 2014;24:210-217.
9. Koritzinsky M, Wouters BG. The roles of reactive oxygen species and autophagy in mediating the tolerance of tumor cells to cycling hypoxia. *Semin Radiat Oncol* 2013;23:252-261.
10. Vaupel P, Mayer A. Tumor oxygenation status: Facts and fallacies. *Adv Exp Med Biol* 2017;977:91-99.
11. Vaupel P. Tumor microenvironmental physiology and its implications for radiation oncology. *Semin Radiat Oncol* 2004;14:198-206.
12. Horsman MR, Sorensen BS, Busk M, et al. Therapeutic modification of hypoxia. *Clin Oncol* 2021;33:e492-e509.
13. Loeffler JS, Durante M. Charged particle therapy—optimization, challenges and future directions. *Nat Rev Clin Oncol* 2013;10:411-424.
14. Karger CP, Peschke P. RBE and related modeling in carbon-ion therapy. *Phys Med Biol* 2017;63:01TR02.
15. Barendsen GW. Responses of cultured cells, tumours, and normal tissues to radiations of different linear energy transfer. *Current Topics in Radiation Research* 1968;4:293-356.
16. Furusawa Y, Fukutsu K, Aoki M, et al. Inactivation of aerobic and hypoxic cells from three different cell lines by accelerated ^{3}He-, ^{12}C- and ^{20}Ne-ion beams. *Radiat Res* 2000;154:485-496.
17. Kamada T, Tsujii H, Blakely EA, et al. Carbon ion radiotherapy in japan: An assessment of 20 years of clinical experience. *Lancet Oncol* 2015;16:e93-e100.
18. Durante M. Heavy charged particles: Does improved precision and higher biological effectiveness translate to better outcome in patients? *Semin Radiat Oncol* 2018;28:160-167.
19. Bassler N, Toftegaard J, Luhr A, et al. Let-painting increases tumour control probability in hypoxic tumours. *Acta Oncol* 2014;53:25-32.
20. Tinganelli W, Durante M, Hirayama R, et al. Kill-painting of hypoxic tumours in charged particle therapy. *Sci Rep* 2015;5:17016.
21. Epel B, Maggio MC, Barth ED, et al. Oxygen-guided radiation therapy. *Int J Radiat Oncol Biol Phys* 2019;103:977-984.
22. Wheeler KT, Deen DF, Leith JT, et al. Cellular response of a rat brain tumor to a therapeutic carbon ion beam. *Radiology* 1979;133:757-760.

23. Tenforde TS, Curtis SB, Crabtree KE, et al. In vivo cell survival and volume response characteristics of rat rhabdomyosarcoma tumors irradiated in the extended peak region of carbon- and neon-ion beams. *Radiat Res* 1980;83:42-56.
24. Hirayama R, Uzawa A, Takase N, et al. Evaluation of SCCVII tumor cell survival in clamped and non-clamped solid tumors exposed to carbon-ion beams in comparison to x-rays. *Mutat Res* 2013;756:146-151.
25. Isaacs JT, Heston WD, Weissman RM, et al. Animal models of the hormone-sensitive and -insensitive prostatic adenocarcinomas, dunning R-3327-H, R-3327-HI, and R-3327-AT. *Cancer Res* 1978;38:4353-4359.
26. Glowa C, Karger CP, Brons S, et al. Carbon ion radiotherapy decreases the impact of tumor heterogeneity on radiation response in experimental prostate tumors. *Cancer Lett* 2016;378:97-103.
27. Peschke P, Karger CP, Scholz M, et al. Relative biological effectiveness of carbon ions for local tumor control of a radioresistant prostate carcinoma in the rat. *Int J Radiat Oncol Biol Phys* 2011;79:239-246.
28. Haberer T, Becher W, Schardt D, et al. Magnetic scanning system for heavy ion therapy. *Nucl Instrum Meth* 1993;A330:296-305.
29. StatSoft Inc. Statistica für windows [software-system für datenanalyse]. www.statsoft.com. Accessed January 8, 2024.
30. Karger CP, Peschke P, Scholz M, et al. Relative biological effectiveness of carbon ions in a rat prostate carcinoma in vivo: Comparison of 1, 2, and 6 fractions. *Int J Radiat Oncol Biol Phys* 2013;86:450-455.
31. Walker AM, Suit HD. Assessment of local tumor control using censored tumor response data. *Int J Radiat Oncol Biol Phys* 1983;9:383-386.
32. Finney DJ. *Statistical Method in Biological Assay*. 3rd ed. Charles Griffin; 1978.
33. Bendinger AL, Glowa C, Peter J, et al. Photoacoustic imaging to assess pixel-based sO_2 distributions in experimental prostate tumors. *J Biomed Opt* 2018;23:1-11.
34. Glowa C, Peschke P, Brons S, et al. Intrinsic and extrinsic tumor characteristics are of minor relevance for the efficacy of split-dose carbon ion irradiation in three experimental prostate tumors. *Radiother Oncol* 2019;133:120-124.
35. Koike S, Ando K, Oohira C, et al. Relative biological effectiveness of 290 MEV/U carbon ions for the growth delay of a radioresistant murine fibrosarcoma. *J Radiat Res* 2002;43:247-255.
36. Tenforde TS, Tenforde SD, Crabtree KE, et al. RBE values for radiation-induced growth delay in rat rhabdomyosarcoma tumors exposed to plateau and peak carbon, neon and argon ions. *Int J Radiat Oncol Biol Phys* 1981;7:217-222.
37. Valable S, Gerault AN, Lambert G, et al. Impact of hypoxia on carbon ion therapy in glioblastoma cells: Modulation by let and hypoxia-dependent genes. *Cancers* 2020;12.
38. Staab A, Zukowski D, Walenta S, et al. Response of chinese hamster v79 multicellular spheroids exposed to high-energy carbon ions. *Radiat Res* 2004;161:219-227.
39. Cartwright IM, Su C, Haskins JS, et al. DNA repair deficient chinese hamster ovary cells exhibiting differential sensitivity to charged particle radiation under aerobic and hypoxic conditions. *Int J Mol Sci* 2018;19.
40. Arai TJ, Yang DM, Campbell 3rd JW, et al. Oxygen-sensitive mri: A predictive imaging biomarker for tumor radiation response? *Int J Radiat Oncol Biol Phys* 2021;110:1519-1529.
41. Zhao D, Constantinescu A, Chang CH, et al. Correlation of tumor oxygen dynamics with radiation response of the dunning prostate R3327-HI tumor. *Radiat Res* 2003;159:621-631.
42. Mena-Romano P, Cheng C, Glowa C, et al. Measurement of hypoxia-related parameters in three sublines of a rat prostate carcinoma using dynamic ^{18}F-FMISO-PET-CT and quantitative histology. *Am J Nucl Med Mol Imaging* 2015;5:348-362.
43. Bayer C, Vaupel P. Acute versus chronic hypoxia in tumors: Controversial data concerning time frames and biological consequences. *Strahlenther Onkol* 2012;188:616-627.
44. Sorensen BS, Horsman MR. Tumor hypoxia: Impact on radiation therapy and molecular pathways. *Front Oncol* 2020;10:562.
45. Eble MJ, Lohr F, Wenz F, et al. Tissue oxygen tension distribution in two sublines of the dunning prostate tumor r3327. In: Vaupel P, Kellerer AM, Gunderoth M, eds. *Tumor Oxygenation: Gustav Fischer Verlag*. Stuttgart: Funktionsanalyse biologischer Systeme; 1995:95-105.
46. Zhao D, Constantinescu A, Hahn EW, et al. Tumor oxygen dynamics with respect to growth and respiratory challenge: Investigation of the dunning prostate R3327-HI tumor. *Radiat Res* 2001;156:510-520.
47. Rich LJ, Seshadri M. Photoacoustic monitoring of tumor and normal tissue response to radiation. *Sci Rep* 2016;6:21237.
48. Michiels C, Tellier C, Feron O. Cycling hypoxia: A key feature of the tumor microenvironment. *Biochim Biophys Acta* 2016;1866:76-86.
49. Butturini E, Carcereri de Prati A, Boriero D, et al. Tumor dormancy and interplay with hypoxic tumor microenvironment. *Int J Mol Sci* 2019;20.
50. Zhang J, Si J, Gan L, et al. Research progress on therapeutic targeting of quiescent cancer cells. *Artif Cells Nanomed Biotechnol* 2019;47:2810-2820.
51. Masunaga S, Ando K, Uzawa A, et al. The radiosensitivity of total and quiescent cell populations in solid tumors to 290 MEV/U carbon ion beam irradiation in vivo. *Acta Oncol* 2008;47:1087-1093.
52. Nakano T, Suzuki Y, Ohno T, et al. Carbon beam therapy overcomes the radiation resistance of uterine cervical cancer originating from hypoxia. *Clin Cancer Res* 2006;12:2185-2190.
53. Scholz M, Kellerer AM, Kraft-Weyrather W, et al. Computation of cell survival in heavy ion beams for therapy. The model and its approximation. *Radiat Environ Biophys* 1997;36:59-66.
54. Kanai T, Furusawa Y, Fukutsu K, et al. Irradiation of mixed beam and design of spread-out bragg peak for heavy-ion radiotherapy. *Radiat Res* 1997;147:78-85.
55. Inaniwa T, Kanematsu N, Matsufuji N, et al. Reformulation of a clinical-dose system for carbon-ion radiotherapy treatment planning at the national institute of radiological sciences, Japan. *Phys Med Biol* 2015;60:3271-3286.
56. Mohamed OAA, Tesen HS, Hany M, et al. The role of hypoxia on prostate cancer progression and metastasis. *Mol Biol Rep* 2023;50:3873-3884.